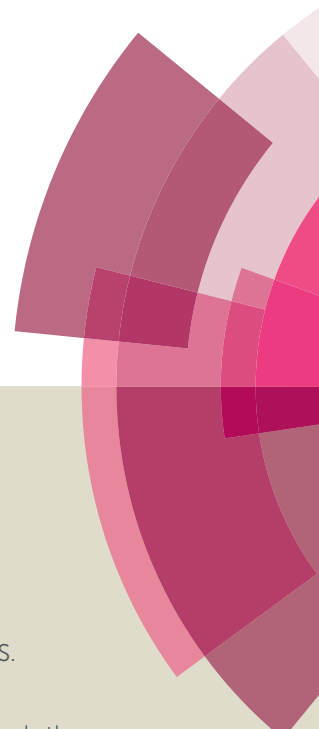


# Journal of Materials Chemistry B

Accepted Manuscript



This article can be cited before page numbers have been issued, to do this please use: K. Han, J. Zhu, S. Wang, Z. Li, S. Cheng and X. Zhang, *J. Mater. Chem. B*, 2015, DOI: 10.1039/C5TB01659B.



This is an *Accepted Manuscript*, which has been through the Royal Society of Chemistry peer review process and has been accepted for publication.

*Accepted Manuscripts* are published online shortly after acceptance, before technical editing, formatting and proof reading. Using this free service, authors can make their results available to the community, in citable form, before we publish the edited article. We will replace this *Accepted Manuscript* with the edited and formatted *Advance Article* as soon as it is available.

You can find more information about *Accepted Manuscripts* in the [Information for Authors](#).

Please note that technical editing may introduce minor changes to the text and/or graphics, which may alter content. The journal's standard [Terms & Conditions](#) and the [Ethical guidelines](#) still apply. In no event shall the Royal Society of Chemistry be held responsible for any errors or omissions in this *Accepted Manuscript* or any consequences arising from the use of any information it contains.



Journal Name

COMMUNICATION

## Tumor targeted gold nanoparticles for FRET-based tumor imaging and light responsive on-demand drug release

Received 00th January 20xx,  
Accepted 00th January 20xxKai Han,<sup>a,b</sup> Jing-Yi Zhu,<sup>a</sup> Shi-Bo Wang,<sup>a</sup> Zi-Hao Li,<sup>a</sup> Si-Xue Cheng<sup>a</sup> and Xian-Zheng Zhang<sup>a,\*</sup>

DOI: 10.1039/x0xx00000x

www.rsc.org/

**In this work, a new type of gold nanoparticles (AuNPs) is designed to achieve the programmed tumor imaging and light manipulated controlled drug release. *In vitro* results demonstrate that these AuNPs undergo matrix metalloproteinase-2 (MMP-2) responsive fluorescence recovery of photosensitizer, protoporphyrin IX (PpIX), in tumor region, which can differentiate tumor cells from healthy ones. Subsequently, the light irradiation activates PpIX, which cleaves the reactive oxygen species (ROS) sensitive thioketal linker, leading to on-demand drug release as well as free drug diffusion into nuclei. More importantly, *in vitro* study indicates the good performance of AuNPs in combined photodynamic therapy and chemotherapy with limited side effects. This AuNPs based nanoplatfrom provides great potential for tumor targeted on-demand combination therapy.**

Satisfactory tumor therapy requires enhanced therapeutic efficacy of drugs with minimized side effects.<sup>1,2</sup> For this purpose, fabrication of intelligent drug delivery vehicles that can release drug on-demand in tumor tissue has attracted great attention during the last decade.<sup>3-5</sup> However, a great many of the existing vehicles encapsulate drugs *via* noncovalent forces, such as hydrogen bonding, hydrophobic or  $\pi$ - $\pi$  stacking interactions.<sup>6-9</sup> These vehicles always suffer from nonspecific drug leakage owing to the poor stability during their circulation in biological systems,<sup>10</sup> which leads to disappointing targeted-therapy with severe systemic toxicity. As an alternative, tumor microenvironmental activatable drug delivery vehicles have been proposed to aim at "zero release" of drugs in normal tissues,<sup>11,12</sup> However, microenvironmental difference between tumor tissues and normal tissues may not be significant enough to differentiate the drug release behavior. For instance, inflammation region was also slightly acid.<sup>13</sup> All these issues highlight the urgency of construction of

well designed nanovehicles to realize on-demand drug release in tumor region.

Recently, imaging guided antitumor therapy provides a new strategy for on-demand therapy.<sup>14-17</sup> For example, Wan *et al.* developed single-walled carbon nanohorns based theranostic agents for photoacoustic imaging guided near-infrared photothermal therapy.<sup>18</sup> Shi *et al.* fabricated organic/inorganic hybrid vesicles for dual-modality imaging-guided high-intensity focused ultrasound ablation.<sup>19</sup> Generally, such a strategy aims at imaging the tumor tissue followed by providing the stimuli to initiate a given therapy. However, these imaging techniques are strongly dependent on fluorescence, thermal, photoacoustic or magnetic resonance imaging (MRI) signals,<sup>20</sup> which are always "on" and constant, regardless of their proximity or interaction with tumor tissues and cells. Consequently, the limited target-to-background signal ratio causes the difficulty in discernment of tumor tissue from the healthy ones. On the other hand, in order to restrict side effects furthest, the therapy modalities are usually limited to local therapies, such as photothermal and ultrasound therapy. Generally, inorganic materials, such as gold nanorods and graphene, but not the chemical drugs were involved in the therapy procedure. However, these local therapies are still far away from practical applications. To our knowledge, chemotherapy dominates antitumor therapy in clinical trials currently. From the standpoint of medicine translation potential, the ideal imaging guided therapy systems should have properties with high resolution of tumor imaging as well as tunable drug release in tumor tissue.

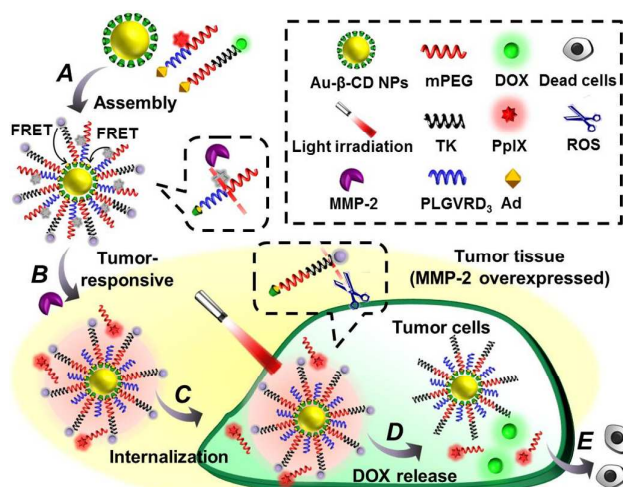
Benefited from the fluorescence "ON/OFF" transformation, fluorescence resonance energy transfer (FRET) technique has been widely used in biomarker detection and imaging with high signal/noise ratio.<sup>21</sup> In particular, FRET-based matrix metalloproteinase-2 (MMP-2) detection and imaging have attracted extensive research interest, since MMP-2 plays key roles in tumor growth, progression, metastasis, as well as dysregulated angiogenesis.<sup>22</sup>

In this study, we designed and fabricated multifunctional AuNPs with MMP-2 responsibility for programmed FRET-based

<sup>a</sup> Key Laboratory of Biomedical Polymers of Ministry of Education & Department of Chemistry, Wuhan University, Wuhan 430072, China. E-mail: xz-zhang@whu.edu.cn

<sup>b</sup> College of Science, Huazhong Agricultural University, Wuhan 430070, China

\*Electronic Supplementary Information (ESI) available: [Experiment details, ESI-MS, and the TGA analysis]. See DOI: 10.1039/x0xx00000x



**Scheme 1** (A) Surface functionalization of Au- $\beta$ -CD NPs *via* host-guest interaction, and both the fluorescence of PpIX and DOX were quenched by Au- $\beta$ -CD NPs *via* FRET; (B) MMP-2 responsive PpIX detachment and imaging in tumor region; (C) cellular internalization of freed PpIX and Au/DOX NPs by tumor cells; (D) light irradiation triggered TK cleavage and on-demand DOX release; (E) apoptosis of tumor cells mediated by chemotherapy and photodynamic therapy.

tumor imaging and light responsive on-demand drug release. As shown in Scheme 1, PEGylated PpIX was conjugated to AuNPs using Pro-Leu-Gly-Val-Arg (PLGVR) peptide sequence as a MMP-2 responsive linker, while doxorubicin (DOX) was anchored on AuNPs through a reactive oxygen species (ROS) sensitive linker, thioketal (TK). Nonfluorescence nanoparticles (denoted as Au/PpIX/DOX NPs) were obtained *via* host-guest interaction. Au/PpIX/DOX NPs that arrived at MMP-2 overexpressed tumor region could liberate quenched PpIX, realizing the tumor tissue imaging. After cellular internalization, light irradiation was performed to break TK linker, which released DOX and ensured the free diffusion to nuclei. This programmed imaging-guided on-demand drug release strategy may allow a combined photodynamic therapy and chemotherapy with improved selectivity and efficiency.

$\beta$ -cyclodextrin-SS ( $\beta$ -CD-SS) modified Au nanoparticles were synthesized (designated as Au- $\beta$ -CD NPs) *via*  $\text{NaBH}_4$  reduction.<sup>23</sup> The structure of  $\beta$ -CD-SS was characterized by electrospray ionization mass spectrometry (ESI-MS, Fig. S1A). Thermal gravimetric analysis (TGA) indicated that the weight loss value of Au- $\beta$ -CD was around 20.0% at 443 °C (Fig. S1B). Transmission electron microscopy (TEM) image revealed that Au- $\beta$ -CD NPs exhibited uniform size around of 7 nm (Fig. 1A). Subsequently, Ac-PEG<sub>3</sub>-K(PpIX)DPLGVRD<sub>3</sub>K(Ad)-CONH<sub>2</sub> and Ad-PEG-TK-DOX were synthesized (Scheme S1, ESI-MS in Fig. S2 and Fig. S3) and mixed with Au- $\beta$ -CD NPs by vigorous stirring. Au/PpIX/DOX NPs with a typical core-shell structure formed *via* host-guest interaction between adamantane (Ad) and  $\beta$ -CD. TEM observation indicated that surface functionalization did not induce observable change in morphology (Fig. 1B). In the current study, the small size of Au- $\beta$ -CD NPs could facilitate the fabrication of Au/PpIX/DOX NPs with good stability *via* the host-guest interaction. In addition, these AuNPs with small size

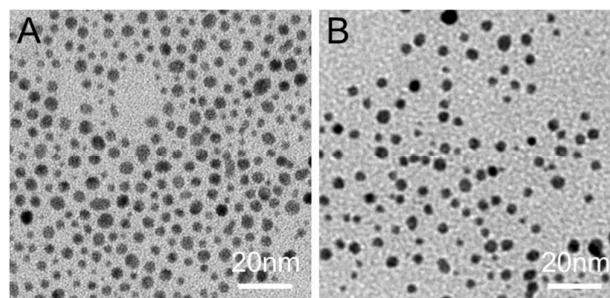


**Fig. 1** TEM images of (A) Au- $\beta$ -CD NPs and (B) Au/PpIX/DOX NPs.

would be beneficial to achieve enhanced sensitivity for tumor biomarkers detection.

To determine the appropriate quencher/fluorophore ratio, the fluorescence quenching and recovery behaviors of Au/PpIX NPs and Au/DOX NPs were studied. Unlike the traditionally fluorescence quenchers which could only quenched limited fluorescent molecules owing to the spectral overlapping efficiency, Au as the quencher has great capability in quenching various fluorophores.<sup>24</sup> As shown in Fig. 2A, the fluorescence of PpIX could be efficiently quenched *via* FRET when the concentration of AuNPs was increased to 7.44 mg/L. Meanwhile, the quenched fluorescence did not increase with prolonging time (Fig. 2C). Once MMP-2 was added, the fluorescence of PpIX increased dramatically (Fig. 2B), indicating the rapidly hydrolysis of PLGVR sequence and detachment of PpIX.<sup>25</sup> These rapid MMP-2 responsiveness was due to the small size of Au/PpIX NPs as mentioned above. Note that  $F_0/F_t$  ratio was nearly 40 when Au/PpIX NPs were incubated with MMP-2 for 4 h (Fig. 2D), suggesting the high PpIX quenching capability and sensitive response to MMP-2. In addition, similar results were found when Au/DOX NPs were incubated with  $\text{H}_2\text{O}_2$ , which was chosen to simulate the ROS environment. Clearly, high sensitive fluorescence OFF/ON phenomenon was observed in Fig. 2E-H, suggesting DOX could be quenched by AuNPs and the thioketal link could be breakdown in the presence of ROS, resulting in the release of DOX.<sup>26</sup>

Subsequently, in order to investigate the feasibility of Au/PpIX/DOX NPs in MMP-2 responsive imaging and light initiated on-demand drug release, the programmed fluorescence recovery of Au/PpIX/DOX NPs under MMP-2 and light irradiation was measured. Au/PpIX/DOX NPs were incubated with MMP-2 for 4 h and subsequently treated by 630 nm light irradiation. It was found that the fluorescence of both PpIX and DOX were quenched well by Au- $\beta$ -CD NPs (6.52 mg/L) (Fig. 2J). Once MMP-2 was added, fluorescence of PpIX increased quickly with time prolonging, while the fluorescence of DOX was unchanged. 4 h later, the solution received 630 nm laser irradiation. As expected, the fluorescence of DOX also increased rapidly (Fig. 2K). It should be pointed out that the fluorescence recovery capability of DOX was lower than that of PpIX to some extent, since the sulfhydrylation of DOX occurred during the breakage of thioketal linker, and the steric hindrance caused by  $\beta$ -CD modification could not prevent the

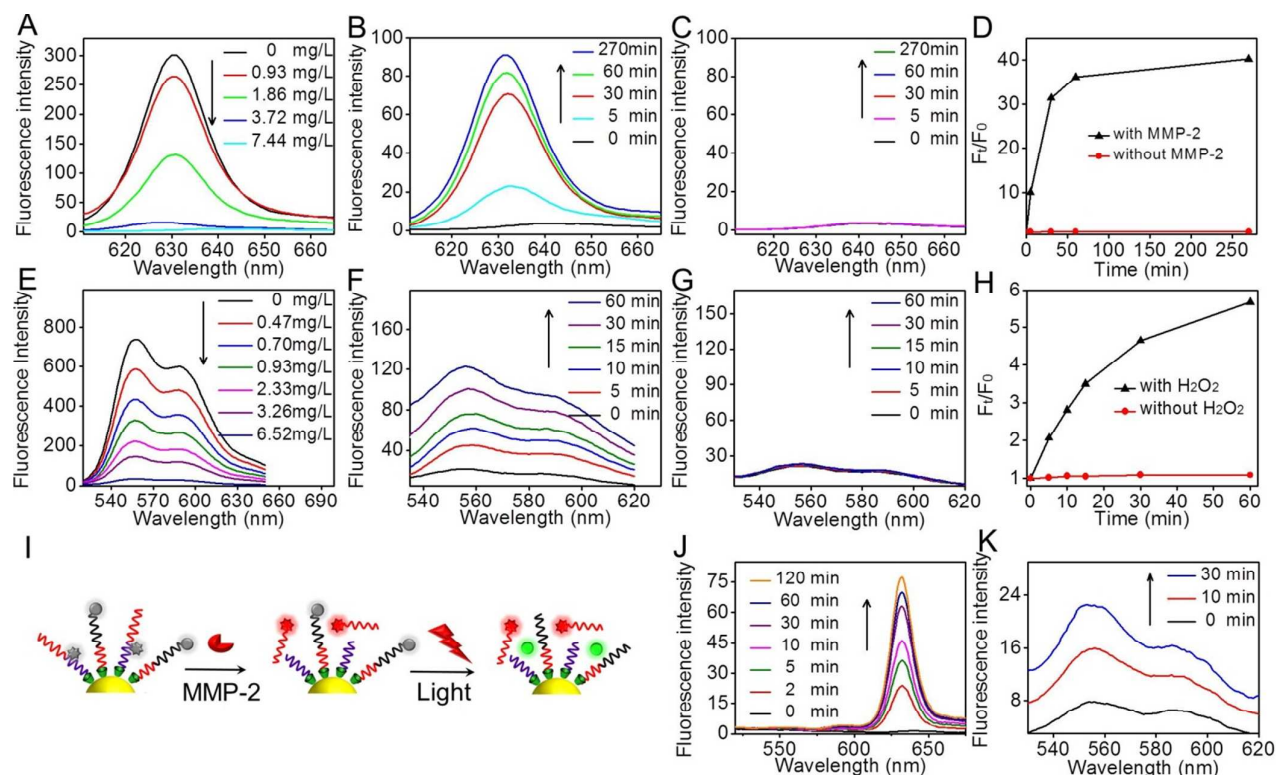


**Fig. 2** Fluorescence quenching behaviors of (A) PpIX and (E) DOX by adding various amounts of Au- $\beta$ -CD NPs. Fluorescence recovery of Au/PpIX NPs (B) in the presence of MMP-2 or (C) absence of MMP-2. Fluorescence recovery of Au/DOX NPs (F) in the presence of H<sub>2</sub>O<sub>2</sub> or (G) absence of H<sub>2</sub>O<sub>2</sub>. F<sub>t</sub>/F<sub>0</sub> ratios of (D) Au/PpIX NPs and (H) Au/DOX NPs with/without corresponding stimulation at preset times. (I) Scheme of the programmed fluorescence recovery. Fluorescence recovery of Au/PpIX/DOX NPs (J) in the presence of MMP-2 and (K) subsequently treated with light irradiation.

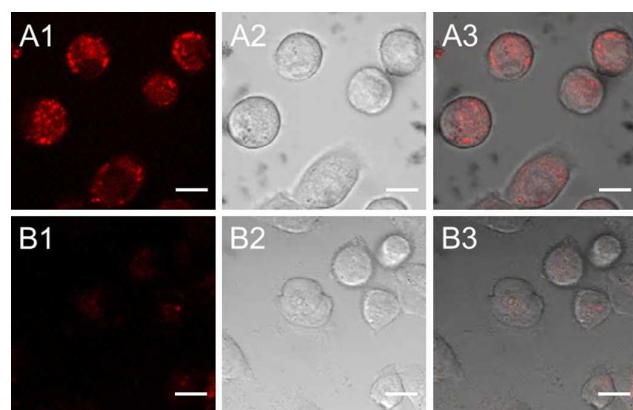


**Fig. 3** MMP-2 responsive fluorescence recovery of Au/PpIX/DOX NPs in (A1-A3) SCC-7 cells and (B1-B3) COS7 cells. Red signal: PpIX; A2 and B2: bright field; A3 and B3: merged field. The scale bar was 10  $\mu$ m while the micrographs were obtained at a magnification of 600 $\times$ .

interaction between Au and sulfhydrylation DOX completely. Taken together, the Au/PpIX/DOX NPs could achieve programmed fluorescence recovery with the stimulation of MMP-2 and light irradiation.

Encouraged by the good MMP-2 responsive fluorescence quenching/recovery ability of Au/PpIX/DOX NPs, we expected that Au/PpIX/DOX NPs could differentiate MMP-2 overexpressed tumor cells from healthy ones, since MMP-2 as

a striking biomarker is upregulated in many types of tumor tissues. The fluorescence recovery of PpIX in cellular level was determined by confocal laser scanning microscope (CLSM). As shown in Fig. 3B1, only extremely low red signal of PpIX was observed in normal COS7 (African green monkey SV40-transfected kidney fibroblast cell line). In contrast, significant PpIX fluorescence was found in SCC-7 (squamous cell carcinoma cell line) (Fig. 3A1). Furthermore, quantitative result of released PpIX was also determined *via* fluorescence spectrum. The contents of released PpIX were  $0.22 \pm 0.02$  mg/L and  $0.08 \pm 0.02$  mg/L in SCC-7 cells and COS7 cells, respectively. SCC-7 cells were known for their high MMP-2 expression. Clearly, the elevated fluorescence intensity and content of PpIX in SCC-7 cells was owing to the hydrolysis of PLGVR peptide sequence by the overexpressed MMP-2, which led to exfoliation of PpIX from Au core as well as the fluorescence recovery. In other words, this fluorescence recovery was realized by recognition of MMP-2 overexpressed tumor cells. More importantly, the recognition of tumor cells could minimize the side effects of photodynamic therapy since ROS and the PDT effect was initiated *via* light irradiation in the tumor region.

To demonstrate that Au/PpIX/DOX NPs possessed capability of on-demand drug release, the fluorescence recovery and cellular localization of DOX were observed *via* CLSM. Au/PpIX/DOX NPs were incubated with SCC-7 cells for 5 h and

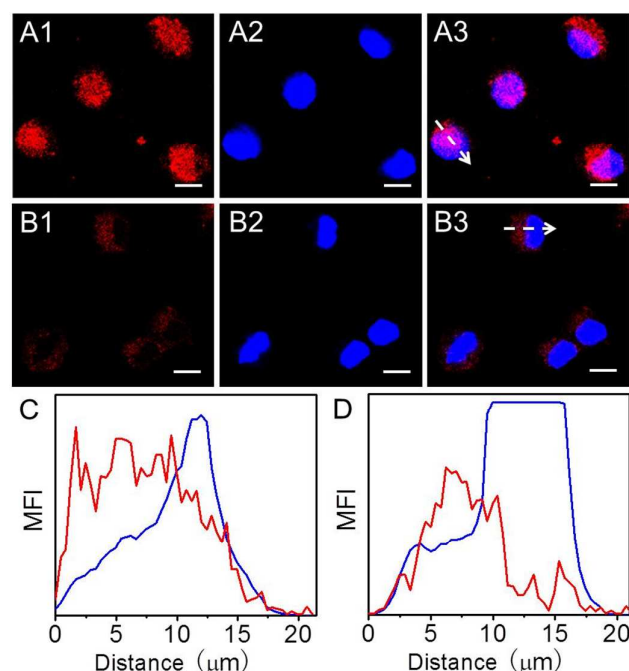


**Fig. 4** Light irradiation mediated fluorescence recovery of DOX when Au/PpIX/DOX NPs were incubated with SCC-7 cells. (A1-A3) SCC-7 cells with 30 min light irradiation; (B1-B3) SCC-7 cells without light irradiation. Red signal: DOX; blue signal: Hoechst 33342; A3 and B3: merged field. The scale bar was 10  $\mu\text{m}$  while the micrographs were obtained at a magnification of 600 $\times$ . Fluorescence intensity profile analysis of DOX (red line) and Hoechst 33342 (blue line) according to (C) A3 and (D) B3, respectively, across the arrowed white line.

then replaced with 10% FBS. Thereafter, SCC-7 cells were treated by 30-min light irradiation and further incubated for 7 h to allow the free diffusion of DOX. As shown in Fig. 4B1, the red signal in SCC-7 cells without light irradiation was very weak, suggesting the DOX could be efficiently quenched by Au- $\beta$ -CD NPs, and the leakage of DOX during endocytosis was negligible. However, when SCC-7 cells were treated by light irradiation, the red signal increased dramatically (Fig. 4A1). It was due to the fact that cleavage of TK linker occurred under light irradiation, leading to the emission of red fluorescence from free DOX. Besides, it was found that part of red fluorescence was overlapped with the Hoechst-stained cell nuclei (Fig. 4A3), indicating free DOX entered cell nuclei. The fluorescence-intensity-profile analysis also confirmed this result in Fig. 4C. In contrast, across the arrowed line in Fig. 4B3, DOX (red line) and cell nuclei (blue line) were basically separated while red signal of DOX was very weak (Fig. 4D). Considering that the nucleus pore was very small, Au/PpIX/DOX NPs could not enter the nuclei with ease. The noninvasive light irradiation manipulation realized on-demand drug release in tumor cells, which would show great advantages in reducing side effects.

Furthermore, MTT assay was determined to evaluate the antitumor therapeutical efficacy of Au/PpIX/DOX NPs. As shown in Fig. 5A, Au/PpIX/DOX NPs exhibited great cytotoxicity in SCC-7 cells when 30-min light irradiation was performed. For comparison, toxicity of Au/PpIX/DOX NPs in COS7 cells was observably decreased. This result was attributed to the

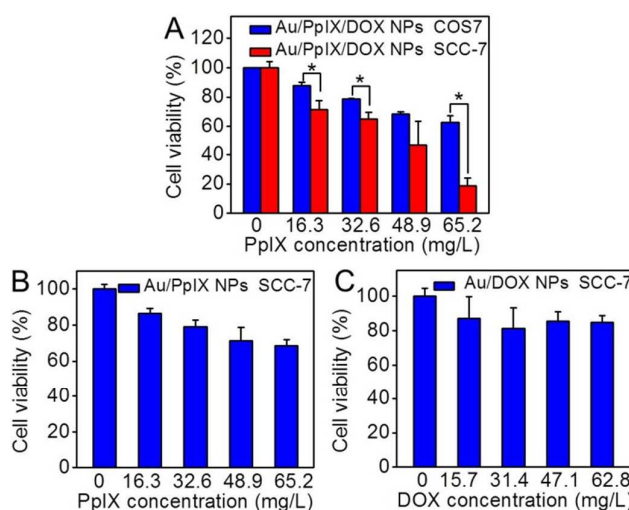


**Fig. 5** (A) Cell viability of Au/PpIX/DOX NPs in COS7 and SCC-7 cells under 30-min light irradiation. (B) Cell viability of Au/PpIX NPs in SCC-7 cells under 30-min light irradiation. (C) Cell viability of Au/DOX NPs in SCC-7 cells. \* $p < 0.05$ , when the group was compared with COS7 cells treated with Au/PpIX/DOX NPs with 30-min light irradiation as determined by a Student's *t*-test.

different MMP-2 expression levels of SCC-7 and COS7 cell-lines ( $3.44 \pm 0.18$  ng/mL and  $0.87 \pm 0.17$  ng/mL in culture medium respectively, which was determined *via* enzyme-linked immuno sorbent assay). As mentioned above, the overexpressed MMP-2 enzyme in culture medium of SCC-7 cells hydrolyzed the PLGVR peptide sequence and released PpIX. After cellular internalization, the following light irradiation not only activated the photodynamic therapeutic efficacy of freed PpIX but also broke down the TK linker, which liberated the quenched DOX and ensured the free access to nuclei.

Since both PpIX and DOX were widely used antitumor drugs, the combination therapy of PpIX and DOX in SCC-7 cells was also evaluated. Au/PpIX NPs and Au/DOX NPs were employed as the controls. As mentioned above, Au/PpIX/DOX NPs exhibited great cytotoxicity. In contrast, although the toxicity of Au/PpIX NPs was dose-dependent (Fig. 5B), the toxicity of Au/PpIX NPs was significantly lower than Au/PpIX/DOX NPs. Meanwhile, Au/DOX NPs had very limited toxicity (Fig. 5C), since the nuclear pore was less than 9 nm,<sup>27</sup> the capability of entering nuclei of Au/DOX NPs was weaker as compared with free DOX, leading to the low toxicity. All these results substantially demonstrated the well tumor targeted combination therapeutic efficacy.

## Conclusions

In summary, we designed and fabricated functional Au/PpIX/DOX NPs for tumor triggered imaging and light manipulated on-demand drug release in tumor cells. These Au/PpIX/DOX NPs realized tumor recognition by MMP-2 responsive PpIX fluorescence recovery. Subsequently, light irradiation liberated of DOX, guaranteeing the free diffusion to nuclei. *In vitro* results indicated that Au/PpIX/DOX NPs

achieved enhanced cell growth inhibition efficiency in MMP-2 overexpressed tumor cells. This programmed tumor imaging and on-demand drug release strategy should show great potential in targeted tumor therapy.

### Acknowledgements

This work was supported by the National Natural Science Foundation of China (51125014, 51233003 and 51273165), the Ministry of Science and Technology of China (2011CB606202), the Natural Science Foundation of Hubei Province of China (2013CFA003).

### Notes and references

- 1 E. K. Lim, T. Kim, S. Paik, S. Haam, Y. M. Huh and K. Lee, *Chem. Rev.*, 2015, **115**, 327.
- 2 Y. Wen and W. S. Meng, *J. Pharm. Innov.*, 2014, **9**, 158.
- 3 C. Li, *Nat. Mater.*, 2014, **13**, 110.
- 4 P. L. Rodriguez, T. Harada, D. A. Christian, D. A. Pantano, R. K. Tsai and D. E. Discher, *Science*, 2013, **339**, 971.
- 5 S. Mura, J. Nicolas and P. Couvreur, *Nat. Mater.*, 2013, **12**, 991.
- 6 Y. S. Zhang, B. Pang, D. C. Hyun, M. X. Yang and Y. N. Xia, *Angew. Chem. Int. Ed.*, 2014, **53**, 12320.
- 7 L. Gu, A. Faig, D. Abdelhamid and K. Urich, *Acc. Chem. Res.*, 2014, **47**, 2867.
- 8 H. Cheng, Y. J. Cheng, S. Bhasin, J. Y. Zhu, X. D. Xu, R. X. Zhuo and X. Z. Zhang, *Chem. Commun.*, 2015, **51**, 6936.
- 9 Y. Wen, H. R. Kolonich, K. M. Kruszewski, N. Giannoukakis, E. S. Gwalt and W. S. Meng, *Mol. Pharmaceutics.*, 2013, **10**, 1035.
- 10 Z. Zhang, L. Wang, J. Wang, X. Jiang, X. Li, Z. Hu, Y. Ji, X. Wu and C. Chen, *Adv. Mater.*, 2012, **24**, 1418.
- 11 J. Lee, H. Kim, S. Han, E. Hong, K. H. Lee and C. Kim, *J. Am. Chem. Soc.*, 2014, **136**, 12880.
- 12 J. Zhang, Z. F. Yuan, Y. Wang, W. H. Chen, G. F. Luo, S. X. Cheng, R. X. Zhuo and X. Z. Zhang, *J. Am. Chem. Soc.*, 2013, **135**, 5068.
- 13 E. A. Mahmoud, J. Sankaranarayanan, J. M. Morachis, G. Kim, and A. Almutairi, *Bioconjugate Chem.*, 2011, **22**, 1416.
- 14 P. Shi, Z. Liu, K. Dong, E. G. Ju, J. S. Ren, Y. D. Du, Z. Q. Li and X. G. Qu, *Adv. Mater.*, 2014, **26**, 6635.
- 15 J. W. Tian, L. Ding, H. X. Ju, Y. C. Yang, X. L. Li, Z. Shen, Z. Zhu, J. S. Yu and C. Y. J. Yang, *Angew. Chem. Int. Ed.*, 2014, **53**, 9544.
- 16 J. Wang, G. Z. Zhu, M. X. You, E. Q. Song, M. I. Shukoor, K. J. Zhang, M. B. Altman, Y. Chen, Z. Zhu, C. Z. Huang and W. H. Tan, *ACS Nano*, 2012, **6**, 5070.
- 17 Y. Y. Yuan, J. Liu and B. Liu, *Angew. Chem.*, 2014, **126**, 7291.
- 18 D. Q. Chen, C. Wang, X. Nie, S. M. Li, R. M. Li, M. R. Guan, Z. Liu, C. Y. Chen, C. R. Wang, C. Y. Shu and L. J. Wan, *Adv. Funct. Mater.*, 2014, **24**, 6621.
- 19 D. C. Niu, X. Wang, Y. S. Li, Y. Y. Zheng, F. Q. Li, H. R. Chen, J. L. Gu, W. R. Zhao and J. L. Shi, *Adv. Mater.*, 2013, **25**, 2686.
- 20 J. Lin, S. J. Wang, P. Huang, Z. Wang, S. H. Chen, G. Niu, W. W. Li, J. He, D. X. Cui, G. M. Lu, X. Y. Chen and Z. H. Nie, *ACS Nano*, 2013, **7**, 5320.
- 21 K. Han, Y. Liu, W. N. Yin, S. B. Wang, Q. Xu, R. X. Zhuo and X. Z. Zhang, *Adv. Healthcare Mater.*, 2014, **3**, 1765.
- 22 D. S. Folk, J. C. Torosian, S. Hwang, D. G. McCafferty and K. J. Franz, *Angew. Chem. Int. Ed.*, 2012, **51**, 10795.
- 23 H. Wang, Y. Chen, X. Y. Li and Y. Liu, *Mol. Pharmaceutics*, 2007, **4**, 189.
- 24 S. Lee, E. J. Cha, K. Park, S. Y. Lee, J. K. Hong, I. C. Sun, S. Y. Kim, K. Choi, I. C. Kwon, K. Kim and C. H. Ahn, *Angew. Chem.*, 2008, **120**, 2846.
- 25 K. Han, Q. Lei, H. Z. Jia, S. B. Wang, W. N. Yin, W. H. Chen, S. X. Cheng and X. Z. Zhang, *Adv. Funct. Mater.*, 2015, **25**, 1248.
- 26 S. H. Lee, M. K. Gupta, J. B. Bang, H. Bae and H. J. Sung, *Adv. Healthcare Mater.*, 2013, **2**, 908.
- 27 F. Alber, S. Dokudovskaya, L. M. Veenhoff, W. Z. Zhang, J. Kipper, D. Devos, A. Suprpto, O. Karni-Schmidt, R. Williams, B. T. Chait, A. Sali and M. P. Rout, *Nature*, 2007, **450**, 695.

COMMUNICATION

Journal Name

Journal of Materials Chemistry B Accepted Manuscript

Published on 14 September 2015. Downloaded by KUNGL. TEKNISKA HOGSKOLAN on 18/09/2015 02:05:18.

## Graphical abstract

Multifunctional AuNPs with MMP-2 responsive tumor imaging and on-demand drug release were designed. Well combined chemotherapy and photodynamic therapy with minimized side effects was realized.

